MAT JOURNALS
Journal of Structural and Transportation Studies
Volume 2 Issue 2

EVALUATION OF EMPIRICAL JOINT SHEAR STRENGTH MODELS FOR SIMULATING DYNAMIC RESPONSES OF REINFORCED CONCRETE STRUCTURES

Basit Issah Alhassan, Jack Osei Banahene * Mark Adom-Asamoah
Department of Civil Engineering, Kwame Nkrumah University of Science and Technology, Kumasi, Ghana
E-mail Id - jobanahene.coe@knust.edu.gh

Abstract

The adequacy of a structural system to withstand earthquake-induced seismic forces is largely dependent on how critical components, particularly joints, are considered at the structural design phase. This becomes heavily important in seismic vulnerability and risk assessment of older-type reinforced concrete structures. The purpose of this study is to evaluate two empirical joint shear models derived from two statistical approaches; Bayesian and nonlinear regression by comparing the responses they give with experimental results. A rigid and zero length rotational spring modelling scheme were implemented in the nonlinear finite element platform Opensees. An exterior beam-column joint sub-assemblage was chosen for a reverse cyclic pushover analysis. The results show that the rigid joint model portrays a much stronger joint than is the case, while the rotational spring model is more representative. While both models give data which resembles the experimental data, the nonlinear regression shear capacity model was better for the selected beam-column joint assemblies. The models show discrepancies in predicting drifts at peak loads, suggesting that they are both conservative.

Keywords: *Shear strength, beam-column joints, earthquake, reinforced concrete*

INTRODUCTION

The integrity of older reinforced concrete structures has become a major subject of study in the structural engineering field. Many research papers have been published on this stability, such as the works of Aycardi, Mander and Reinhorn (1995) and Bracci, Reinhorn and Mander (1996). Many existing mid-1970s, reinforced concrete buildings are considered as inadequate when it comes to earthquakes. It is preferred that the analysis of beam-column joints in older RC frame buildings recognizes the flexibility of the joints.

The main method used to address the problem of joint flexibility, is to identify possible parameters which may influence joint shear strength in particular and then, using experimental test results and analytical procedures, confirm which parameters actually have influence on joint behavior. The implementation of joint models in the analytical procedures of old RC frame buildings involves 3 components; a mechanical model (either a single component or multicomponent), a shear capacity backbone curve and a hysteretic response rule which defines cyclic behavior. Several shear capacity backbone curves defined by different parameters are reported in literature. However, there is no consensus about the effect and use of these parameters, and thus different studies come up with different model parameters.

This paper first and foremost reviews some joint shear capacity prediction models and some joint shear behaviour

modelling approaches. The influence of different backbone curves on inelastic rotational RC beam-column joint behaviour is evaluated by two empirical joint shear models derived from two statistical approaches; Bayesian and nonlinear regression by comparing the responses they give with experimental results. This will be obtained by validating a Bayesian joint shear model by Kim and LaFave (2009) and a nonlinear regression model by Jeon (2013), both of which were originally derived using the same influential design parameters for comparison.

REVIEW OF JOINT SHEAR CAPACITY MODELS

Kim and LaFave (2009) characterised the joint shear behaviour of reinforced concrete beam-column connections that are subjected to seismic lateral loads. By assembling a database of previously tested beam-column joint sub-assemblages in literature, 10 influential parameters were identified to help determine their joint shear capacities. They are put through a Bayesian removal process, in which they are removed one by one, and the results of the equation examined to determine whether their removal affects those results or not. A positive response or change indicates that the parameter in question is important towards the equation. After the removal procedure and a series of analyses, a practical design expression was proposed (see Equation 1).

$$v_j(MPa) = \alpha_r \beta_r \lambda_r \eta_r (JI)^{0.15} (BI)^{0.30} (f_c')^{0.75} \quad (1)$$

where α_r is a parameter for describing in-plane geometry: 1.0 for interior connections, 0.7 for exterior connections, and 0.4 for knee connections; β_r is a parameter for describing out-of-plane geometry: 1.0 for subassemblies with 0 or 1 transverse beams and 1.18 for subassemblies with 2 transverse beams; η_r describes joint eccentricity (equals 1.0 with no joint eccentricity); and λ_r is 1.02. This simple and unified model maintains an acceptable level of dependability as compared to earlier formulated equations during the model development, and it is almost entirely neutral in estimating joint shear strength.

Jeon (2013) also developed a joint shear capacity model as part of his study on aftershock vulnerability assessment of damaged reinforced concrete columns. Similar to the work of Kim and LaFave (2009), Jeon (2013) also considered the 10 selected influential design parameters used for quantifying joint shear strength, but however adopted the frequentist approach (multivariate nonlinear regression analysis) for parametric estimation purposes. To determine the parameters which truly affect the results of the model, stepwise regressions are done until all insignificant ones are eliminated. Analysis of variance tests are conducted at each stage to aid in this as well. The parameters which have a p-value less than or equal to 0.05 qualify as statistically significant, and all others are removed from the equation. The final joint shear strength model for non-ductile beam-column joint was proposed as in Equation 2.

$$V_{\max}(MPa) = 0.586(TB)^{0.774}(BI)^{0.495}(JP)^{1.250}(f_{cj})^{0.941} \quad (2)$$

Other existing research works on the estimation of joint shear capacity models for reinforced concrete structures that were not evaluated in this study are also discussed briefly below.

Attaalla and Agbabian (2004) suggested an analytical equation to estimate joint shear strength for interior and exterior beam-column joints. The proposed equation reflects most significant parameters that influence the joint behaviour (such as axial forces in the beam and column, horizontal and vertical joint reinforcement ratios, and

geometry), whilst accounting for the compression-softening phenomenon associated with cracked reinforced concrete. For the model validation, 69 exterior and 61 interior beam-column joints are used, all of which are specimens experiencing joint shear failures with or without beam yielding.

Park and Mosalam (2012) proposed a strut-and-tie model to predict the joint shear strength of exterior beam-column joints without transverse reinforcement which experienced joint shear failures with and without beam yielding. The proposed joint shear strength model accounted for joint aspect ratio and beam reinforcement ratio. Although their model can predict the joint shear strength for non-ductile exterior and corner joints well, their proposed formulation cannot be applied to interior or roof joints. In order to overcome the limitation of the applicability to other joint types, Park *et al.* (2013) modified the joint shear strength model proposed by Park and Mosalam (2012) by employing simple modification factors to the exterior joint shear strength coefficient. Although analytical predictions provide reasonable results through the comparison of fitted responses and experiment results, actual joint strength coefficient ratio based on experimental observation is different for roof and interior joints.

Hassan (2011) suggested an empirical bond strength model to evaluate the joint shear strength for exterior and corner joints with the short embedment length of beam bottom reinforcement. The bond strength equation includes axial load, beam bar diameter, cover to bar diameter, cover to bar diameter ratio, and the presence of transverse beams to improve existing bond strength models. Using the proposed equation and equilibrium, the equivalent joint shear strength associated with bond failure was derived and compared with 21 experimental results. The mean and coefficient of variation of the ratio of experimental and calculated joint shear strength coefficient are 0.94 and 0.14, respectively. The proposed equation is only applicable for the case of pull-out failure before rebar yielding.

REVIEW ON MODELLING JOINT SHEAR BEHAVIOUR

Lowes and Altoontash (2003) proposed a four-node 12-DOF joint element that consists of eight zero-length bar slip springs, four interface shear springs, and a panel that deforms only in shear. Because of limited research on the bond-slip data of full-scale frames or beam-column joint sub assemblages, the monotonic and cyclic response of the bar stress-slip relationship were developed from experimental studies of anchorage-zone specimens and based on the assumption that bond stress within the joint is constant or piecewise constant. To define the backbone curve of the shear panel, the MCFT was utilized. The cyclic response of the panel zone was modelled by a highly pinched hysteresis relationship. A relatively stiff elastic load-deformation response was assumed for the interface-shear elements.

Mitra (2007) subsequently evaluated the model developed earlier by Lowes and Altoontash (2003) by comparing the simulated response with the experimental response of beam-column joint sub assemblages. The experimental data used for the model validation included interior specimens with at least a minimal amount of joint transverse reinforcement. Therefore, the model may not capture the hysteretic response for joints with little or no joint transverse reinforcement. Mitra (2007) demonstrated that in joints with low amounts of transverse reinforcement, shear is transferred primarily through a compression strut, a mechanism, which is stronger and stiffer than predicted by the MCFT.

Altoontash (2004) simplified the model proposed by Lowes and Altoontash (2003) by introducing a model consisting of four zero-length bar-slip rotational springs located at beam and column-joint interfaces and a zero-length joint rotational spring at an internal node. The constitutive relationship of the shear panel follows the model of Lowes and Altoontash (2003). To alleviate the limitation of the MCTF for joints with no transverse reinforcement, the calibration of constitutive parameters was still required. Altoontash (2004) modified the beam or column fibre sections to represent the bar pull-out mechanisms based on the assumption that the development length is adequate to prevent complete pull-out. However, this assumption is not necessarily true for joints with discontinuous beam bottom reinforcement. The validation was performed for interior beam-column joint sub assemblages and a 0.7 scale two-story RC frame.

The aforementioned joint models (Lowes and Altoontash (2003), Mitra (2007), and Altoontash (2004)) were developed employing the MCFT to define the backbone curve of a joint panel. However, the review of the previous models demonstrates that the MCFT approach is not appropriate to predict the shear strength for non-ductile joints with insufficient joint transverse reinforcement. Additionally, MCFT may underestimate the joint shear strength for such joints. Therefore, the MCFT can provide the reasonable estimate of joint shear strength for ductile joints while the application of the MCFT to non-ductile joints requires additional modifications.

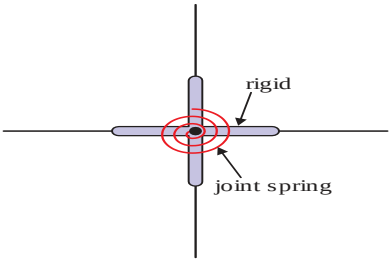

(a) Alath and Kunnath (1995)

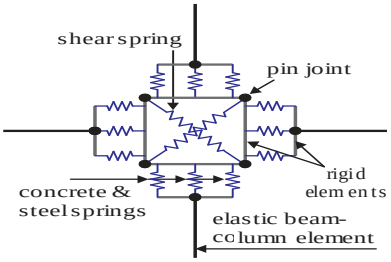

(b) Youssef and Ghobarah (2001)

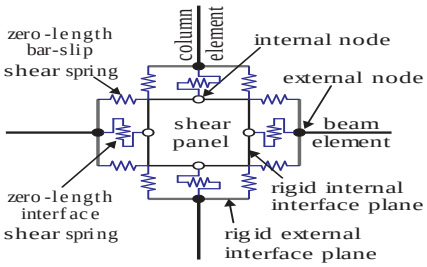

(c) Lowes and Altoontash (2003)

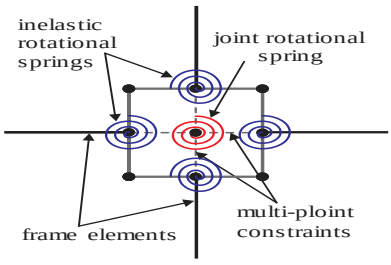

(d) Altoontash (2004)

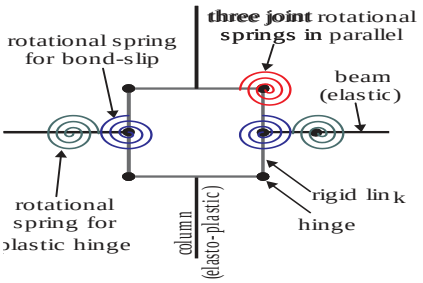

(e) Shin and LaFave (2004)

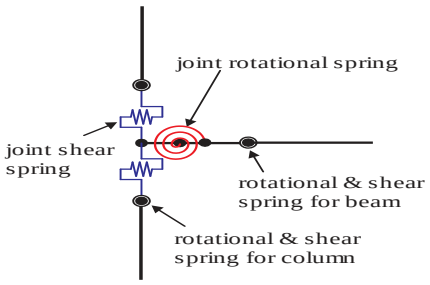

(f) Sharma et al. (2011)

Fig 1. *Existing beam-column joint model idealization*

Celik and Ellingwood (2008) developed a non-ductile joint model based on experimental determination of joint panel shear stress-strain relationship, with inclusion of the bond stress of insufficient beam bottom reinforcement anchorage. The backbone curve of the joint is a quad-linear curve consisting of four key points: concrete cracking, member yielding, ultimate, and residual conditions. Thus, this proposed approach is limited to the case when shear failure occurs after beam yielding. Ordinates on the backbone curve of the joint were computed through moment-curvature analyses for members adjacent to the joint. Then, the joint shear strength was adopted as the smallest of experimental and analytical values. Furthermore, the damage pinching parameters of the joint were not addressed, and therefore their model underestimates the joint shear and overall deformation for the case of joints experiencing a highly pinched hysteresis.

From the proposals above, the mechanics-based or empirical-based joint model is limited to a specific joint type (interior or exterior as well as non-ductile or ductile). Therefore, a unified joint shear model that can be simply and properly applied to various joint types is required when creating the analytical frame model.

METHODOLOGY

Three test units were chosen from the work of Pantelidis (2002). They were all full scale models of typical exterior beam-column joints found in the US before 1970. The reinforcement was modified (increased) in order to ensure that the failure mode in the joint would be shear failure. The joints themselves are non-ductile (i.e. no transverse reinforcements in the joints).

Materials

Concrete

Initial design was for a concrete compressive strength of 27.6 MPa. Care was taken to ensure that the batches met the mix design so that all the test units had strength that were close in value. Table 1 below shows the compressive strength of each test unit:

Table 1 *Concrete compressive strength of test units*

Test Unit	Compressive strength(MPa)
1	30.2
2	31.6
3	31.6

Steel Reinforcement

The main sizes of reinforcement used are shown in Table 2 below along with their ultimate and yield strengths.

Table 2. *Steel reinforcement strength*

Reinforcement Type	Bar Size	F_u (ksi)	F_y (ksi)
Beam longitudinal	9	110.4	66.5
Column longitudinal	8	107.6	68.1
Stirrups/Ties	3	94.9	62.0

Construction of Test Units

All three units were constructed with the same dimensions and similar detailing. The difference lied in how the longitudinal reinforcement were embedded in the

column, as will be visible in Figures 2, 3 and 4 directly below:

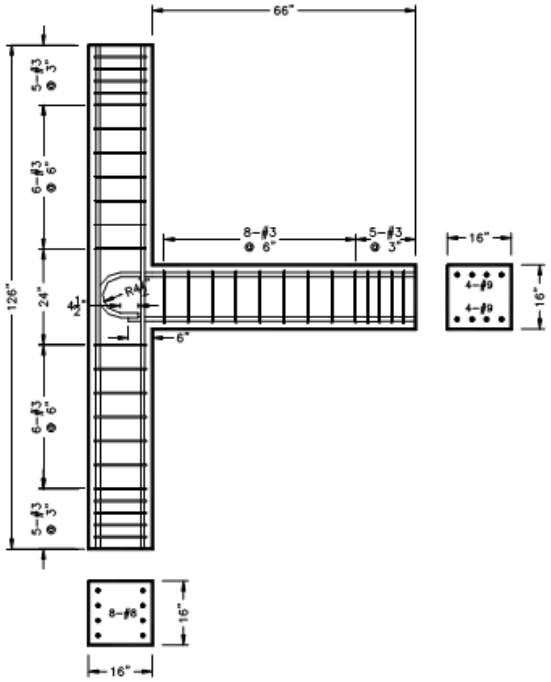

Fig 2. *Dimensions and detailing of test unit 1*

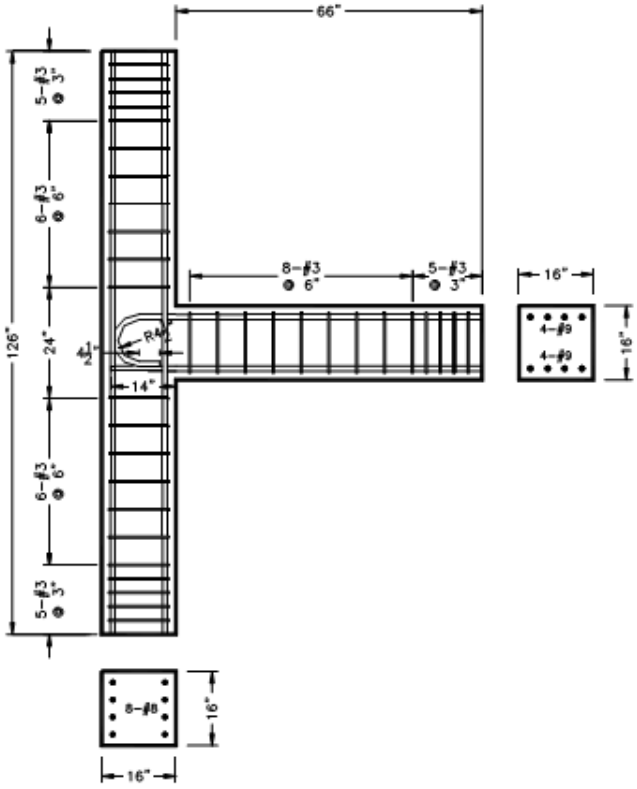

Fig 3. *Dimensions and detailing of test unit 2*

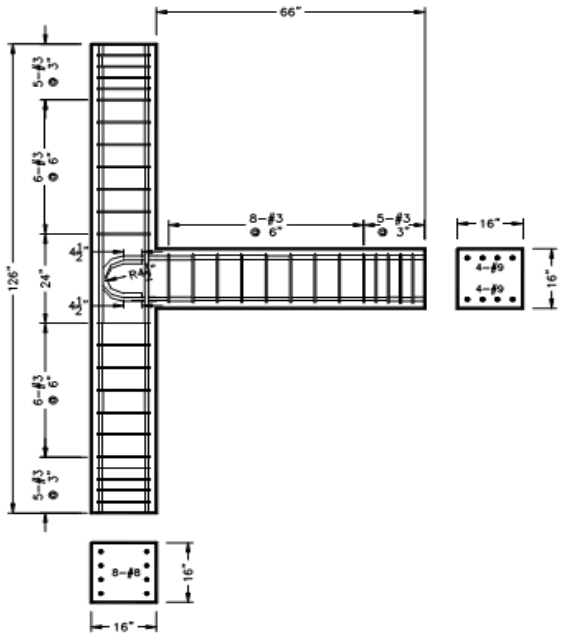

Fig 4. *Dimensions and detailing of test unit 3*

The dimensions of beams for all three test units are 16 inches by 16 inches. Longitudinal reinforcement consists of 4 #9 bars at both top and bottom. The transverse reinforcement consists of two stirrups per section, spaced at 6 inches along the beam, but then reduces to 3 inches within 15 inches of the beam end. It is in this range that it is expected that the shear forces will be maximized and so the reduced spacing is designed to give adequate strength. See Figure 5 for the beam cross section.

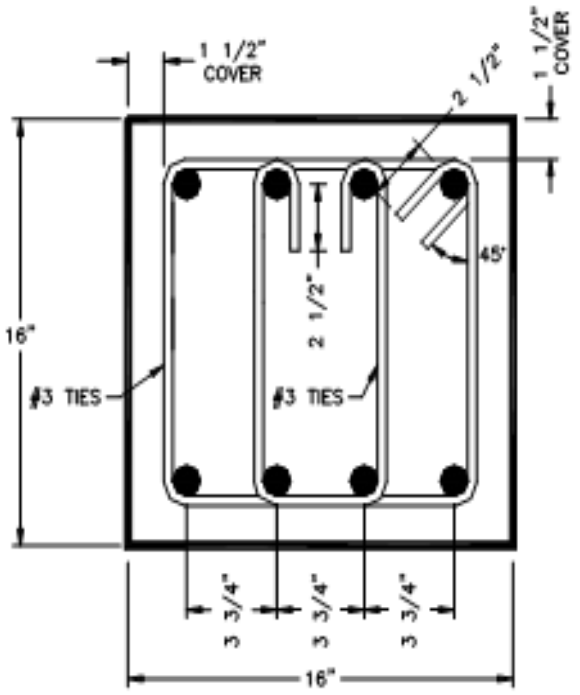

Fig 5. *Beam cross section*

The column dimensions for all the units are 16 inches by 16 inches. Longitudinal reinforcement consists of 4 #8 bars on the beam-column face and 4 #8 bars on the opposite face[1-5]. The transverse reinforcement consists of two stirrups per section, spaced at 6 inches along the column, except within the joint region, where there is no transverse reinforcement. Spacing reduces to 3 inches at the top and bottom of the column. See Figure 6 below for the column cross section.

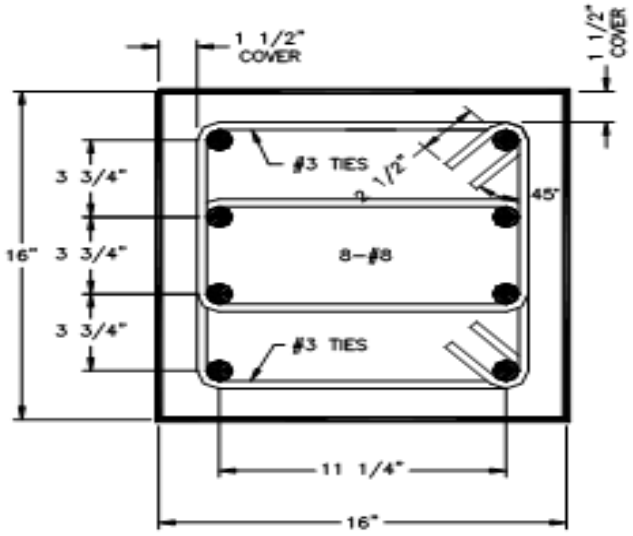

Fig 6. *Column cross section*

Test Procedure and Joint Modelling

The columns were pinned at both ends and an axial load factor of 0.25 applied to it. The loading protocol, as outlined by Pantelidis (2002), consisted of displacement-controlled steps of 0.25%, 0.50%, 0.75%, 1.0%, 1.5%, 2.0%, 3.0%, 5.0%, 7.0% and 9.0% drift.

The computer program Opensees (McKenna, 2010) was used as a computational platform in order to implement joint models in the dynamic analyses of the RC frames. Appropriate material models and elements were employed in the beam-column joint element formulation whilst considering material and geometric nonlinearities usually applied to beams and columns (Adom-Asamoah and Osei, 2016). The hysteretic response was simulated using the "Pinching4" material model (Figure 7) subjected to the shear zone of zero length rotational spring of the so-called "scissors model".

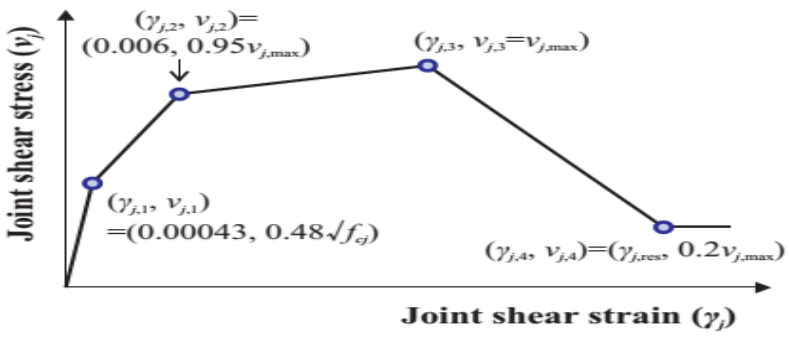

Fig 7. *Backbone curve for pinching4 material*

This backbone curve has four main points along which lines are drawn, whose coordinates are largely dependent on joint shear strength calculations from the predicted data obtained using the model of Kim and LaFave (2009) and Jeon (2013) (see Table 4 and 5).

Table 4. *Calculations on joint shear strength based on model of Kim and Lafave (2009)*

Test Unit	A	β	η	Λ	JI	BI	fc'(MPa)	vj(MPa)	vj(ksi)
1	0.700	1.000	1.000	1.020	0.0139	1.080	30.2	4.956	0.7183
2	0.700	1.000	1.000	1.020	0.0139	1.080	31.6	5.127	0.7431
3	0.700	1.000	1.000	1.020	0.0139	1.080	31.6	5.127	0.7431

Table 5. *Calculations on joint shear strength based on model of Jeon (2013)*

Test Unit	TB	BI	JP	Fc	Vmax (MPa)	Vmax (ksi)
1	1.03	0.22	0.84	30.2000	5.623	0.8149
2	1.03	0.22	0.84	31.6000	5.868	0.8504
3	1.03	0.22	0.84	31.6000	5.868	0.8504

The pinching4 material is applied as a response backbone with an unload-reload path and three damage rules: unloading stiffness degradation, strength degradation, and reloading strength degradation. The response curve is shown below in Figure 8:

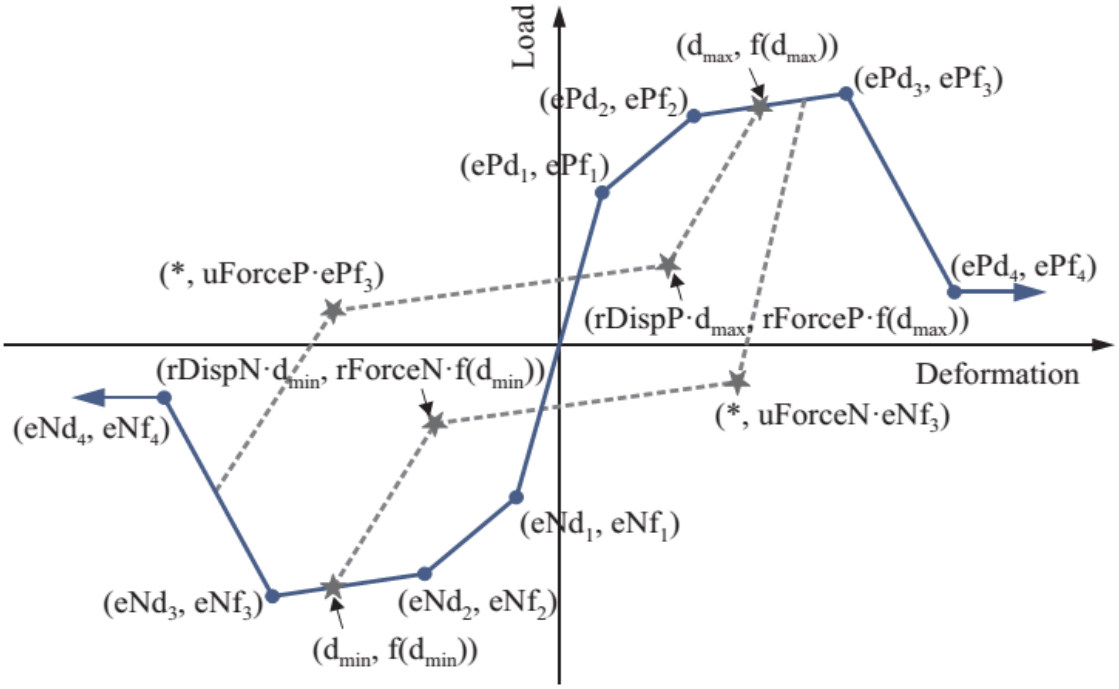

Fig 8. *Response model proposed by Lowes and*

RESULTS AND DISCUSSIONS

The beam and column moment capacity were determined using a script in Opensees to run a moment-curvature analysis on their respective sections. See Table 6 for the values and their experimental counterparts:

Table 6. *Comparison of Predicted and Computed Section Properties*

Test Unit	Axial Load (kips)	Beam Moment Capacity (kip-in)		Column Moment Capacity (kip-in)	
		Predicted	Computed	Predicted	Computed
1	307	3024	3073	3120	2996
2	316	3024	3085	3168	3096
3	294	3024	3034	3084	2790

The computed parameters were all obtained by using the specific strengths and other properties for each test unit. The significance of the computation and subsequent comparison is to ensure that the constructed sections adequately represent the actual test units in digital form[6-11].

Comparison of Experimental Results with Simulated Rigid Joint Models

In order to compare the results from both approaches, a graph of applied lateral load on the beam against drift (a ratio of displacement to member length) of the beam tip must be plotted and the shapes and values analysed. However, as has been mentioned earlier, the rigid joint model is suspected to be inadequate in terms of representing the exact behaviour of the joints of the test units[12-14]. The closeness of the two plots (i.e. the experimental and rigid model) should give an indication of whether this suspicion is accurate or not. Figure 9 and 10 represent the graphs for test unit 1; Figure 11 and 12 represent the graphs for test unit 2; Figure 13 and 14 represent the graphs for test unit 3.

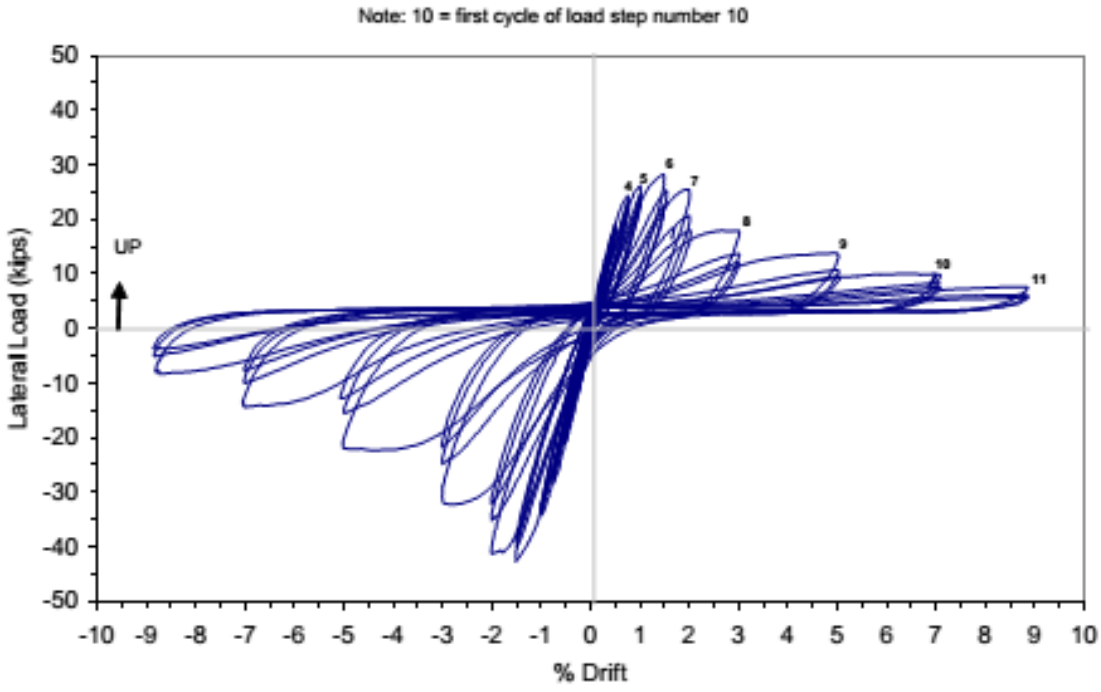

Fig 9. *Lateral load-Drift graph of experimental data for test unit 1*

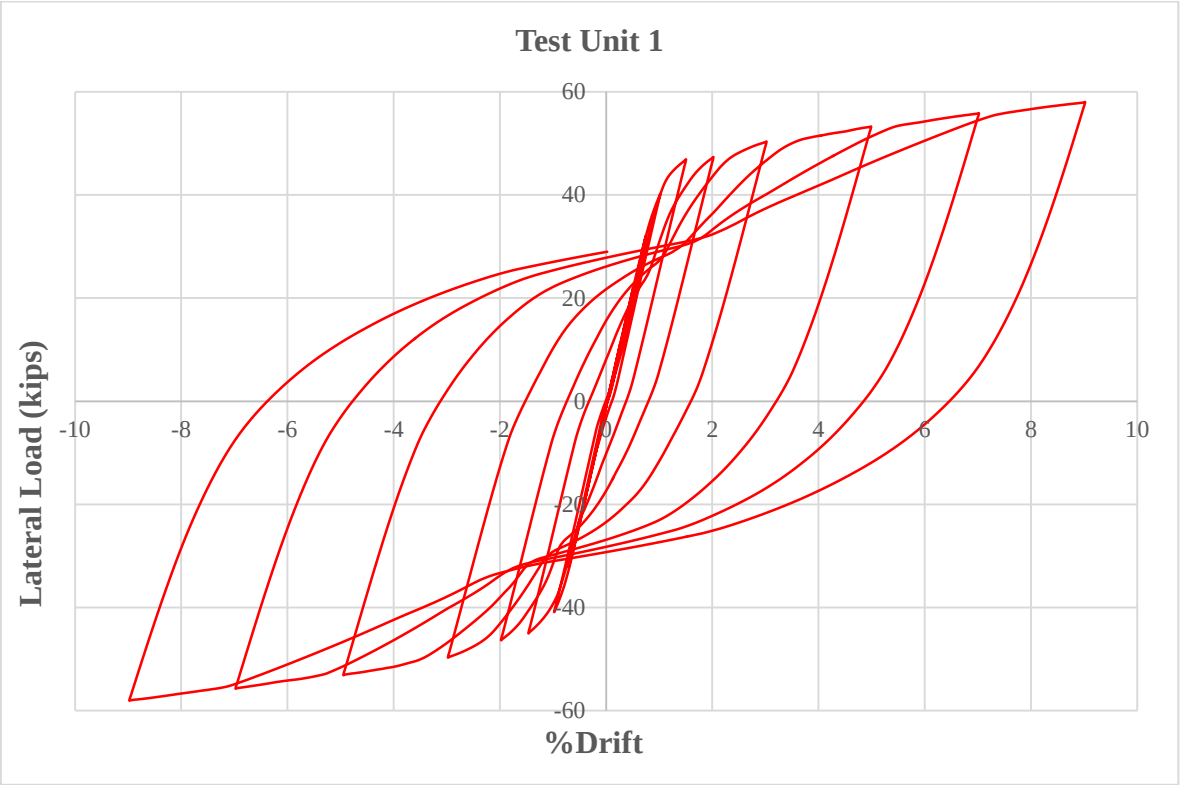

Fig 10. *Lateral load-Drift graph of rigid model for test unit 1*

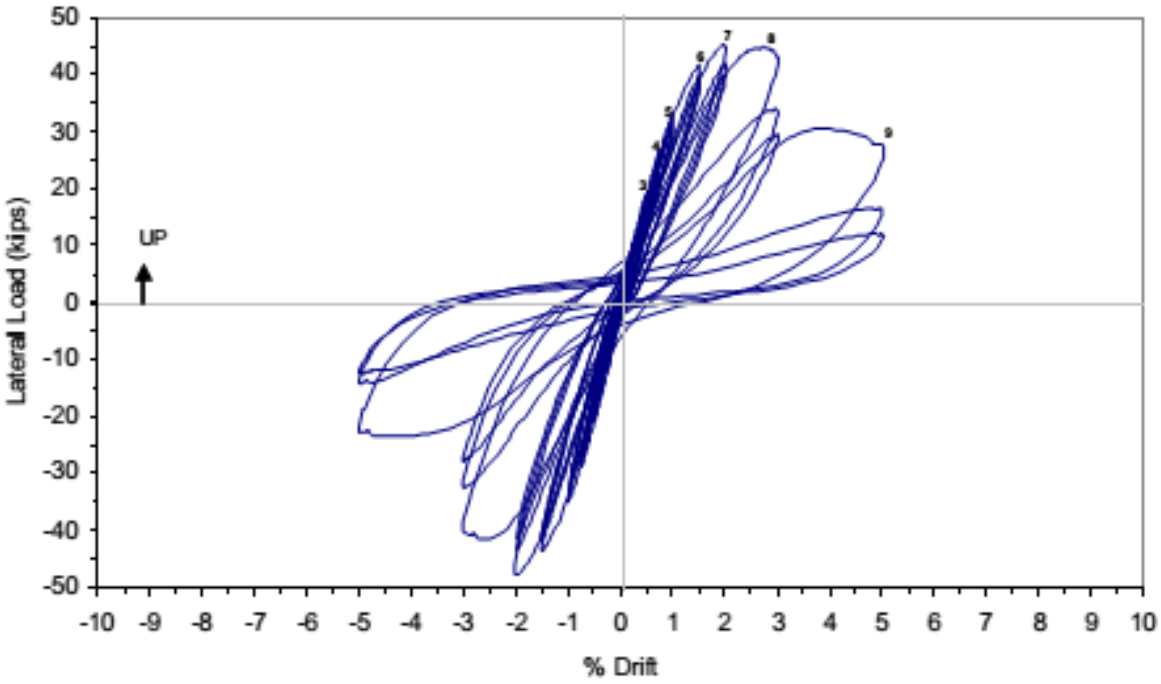

Fig 11. *Lateral load-Drift graph of experimental data for test unit 2*

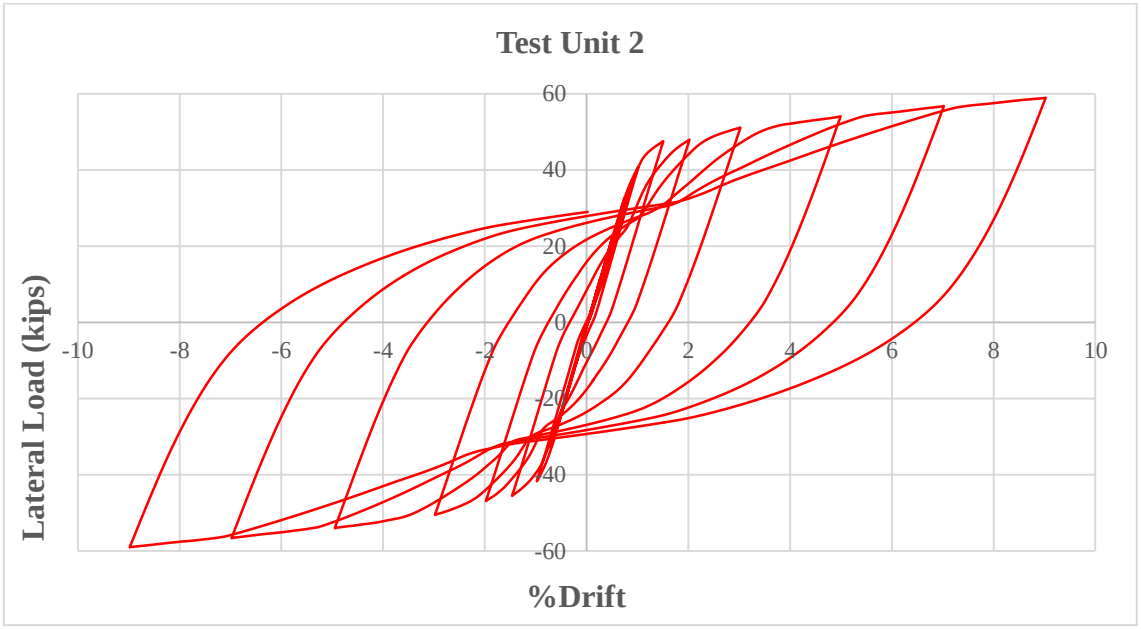

Fig 12. *Lateral load-Drift graph of rigid model for test unit 2*

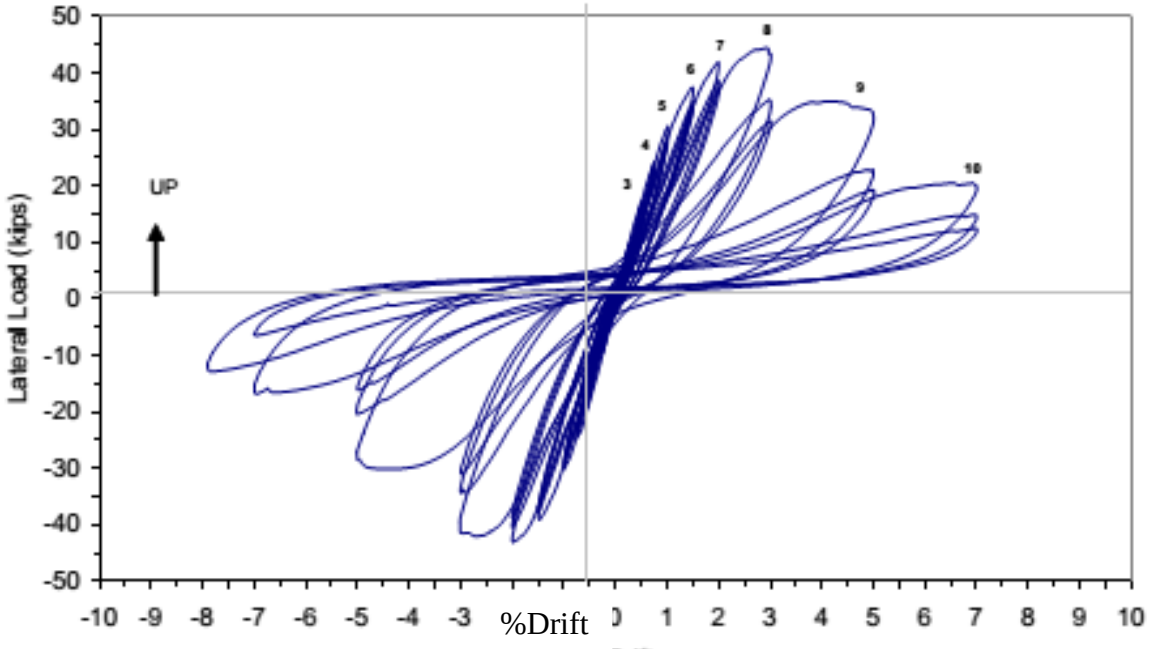

Fig 13. *Lateral load-Drift graph of experimental data for test unit 3*

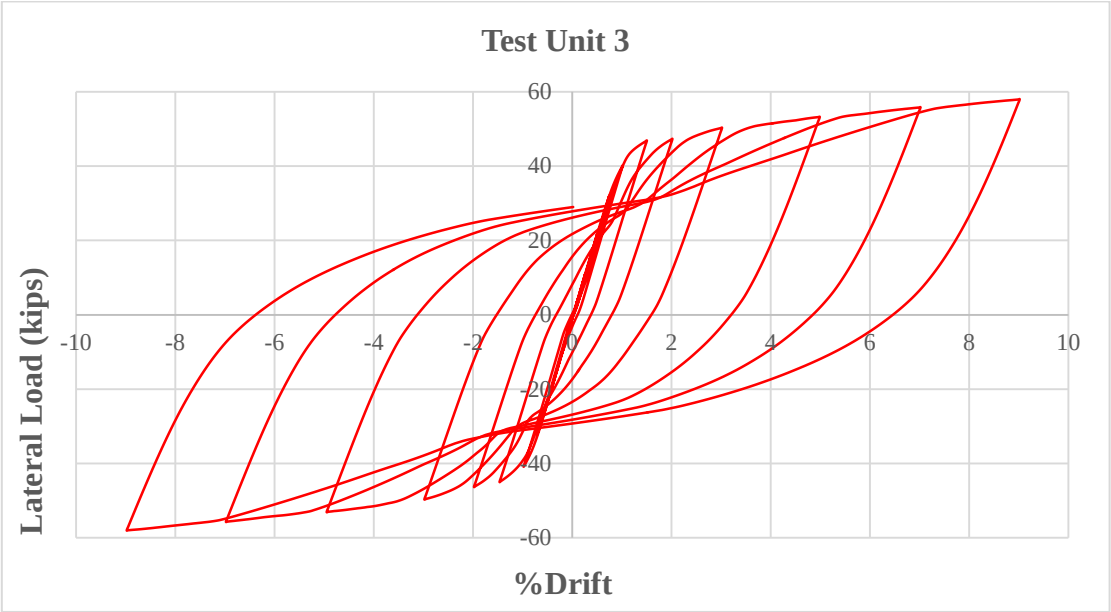

Fig 14. *Lateral load-Drift graph of rigid model for test unit 3*

The hysteretic plots from the rigid model are not close to the experimental plots, indicating that the rigid model is far from adequate in representing the inelastic and pinched nature of the test unit. The peak lateral loads in both upward and downward directions for the rigid models hover around 58kips, at about 9.0% drift for the simulated rigid model. Comparing them to their experimental counterparts, the values for the rigid model are significantly higher, as the experimental test unit peaked at 50kips. This raises the need for a more accurate representative model. For our study, a rotational spring model has been selected.

Comparison of Experimental Results with Simulated Responses from Opensees rotational spring model

Lateral loads and corresponding drifts of the tip of beam tested for the zero-length rotational spring model implemented are obtained.

The same comparison is made between plots from the Opensees model and the experimental results. The activation of the pinching4 material, as mentioned above, depends on the predicted joint shear strength provided by the models used in this study (i.e. Kim and LaFave (2009) and Jeon (2013)).

It should also be noted that the graphs provided by the rotational spring model, unlike the rigid model, resemble the experimental graphs, with the difference being that where the experimental graphs provide more curved lines, the rotational spring model gives trilinear curves, which give a more scissor-like appearance.

Test Unit 1

The plot (Figure 15) seen below shows the lateral load against drift as simulated by Opensees with a rotational spring joint model. It is easy to notice that both graphs somewhat resemble the experiment data in Figure 9. The upward direction resistance is much smaller compared to that in the downward direction, mainly due to the inadequate embedment of the bottom bars in the column joint (6 inches). In order to keep the difference between the upward and downward loads, the ratio between their peaks (1.51) was noted and applied in the stress-strain backbone curve of the pinching4 material.

The comparison of the maximum loads in either direction between the three of the

experimental data, the data from the Kim and LaFave (2009) model and that from the Jeon (2013) model can be found in Table 7 below:

Table 7. *Comparison of load and drift values obtained from both models to experimental values for test unit 1*

	Upward Direction Maximum Load (kips)	%Drift	Downward Direction Maximum Load (kips)	%Drift
Experiment	28.30	1.48	42.70	1.52
Kim and Lafave (2009)	25.30	2.92	38.40	2.88
Jeon (2013)	28.97	3.02	44.28	3.38

By comparison, the values provided by Jeon (2013) joint shear strength prediction model are significantly closer to the experimental data.

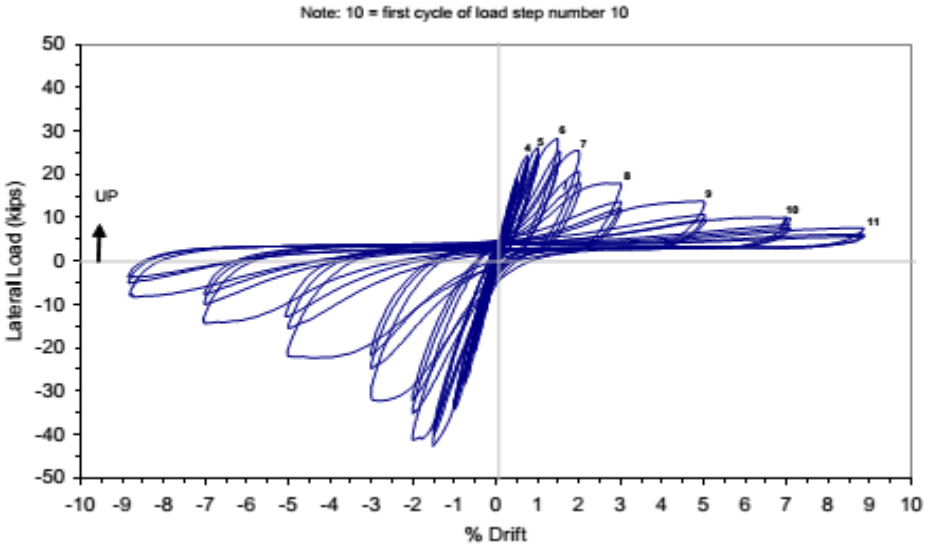

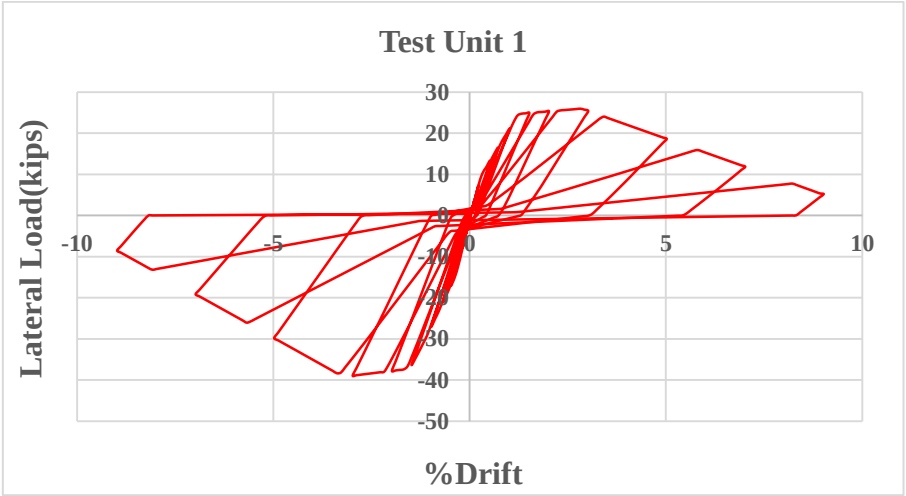

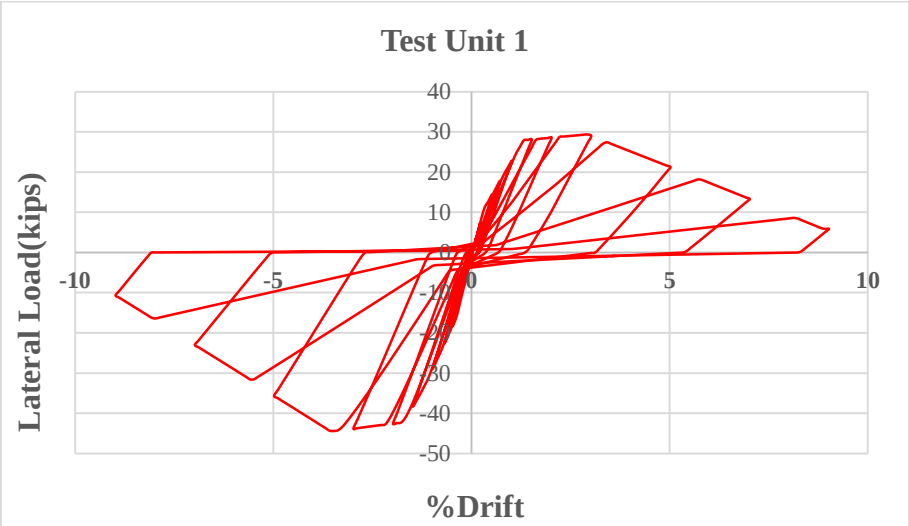

Fig15. *Comparison of the graphs from the experimental data (top), data produced from the Kim and LaFave (2009) model (middle) and the data produced from the Jeon (2013) model (bottom) for test unit 1*

Test Unit 2

The plot (Figure 16) seen below shows the lateral load against drift as simulated by Opensees with a rotational spring joint model. It is easy to notice that both graphs somewhat resemble the experiment data in Figure 11. The upward direction resistance is only slightly smaller compared to that in the downward direction, mainly due to the adequate embedment of the bottom bars in the column joint (14 inches). In order to keep the difference between the upward and downward loads, the ratio between their peaks (1.05) was noted and applied in the stress-strain backbone curve of the pinching4 material.

The comparison of the maximum loads in either direction between the three of the experimental data, the data from the Kim and LaFave (2009) model and that from the Jeon (2013) model can be found in Table 4.3 below:

Table 8. *Comparison of load and drift values obtained from both models to experimental values for test unit 2*

	Upward Direction		Downward Direction	
	Maximum Load (kips)	%Drift	Maximum Load (kips)	%Drift
Experiment	45.10	2.00	47.50	2.00
Kim and Lafave (2009)	38.32	2.92	40.28	2.88
Jeon (2013)	44.02	3.72	46.15	3.78

By comparison, the values provided by the Jeon (2013) joint shear strength prediction model are significantly closer to the experimental data.

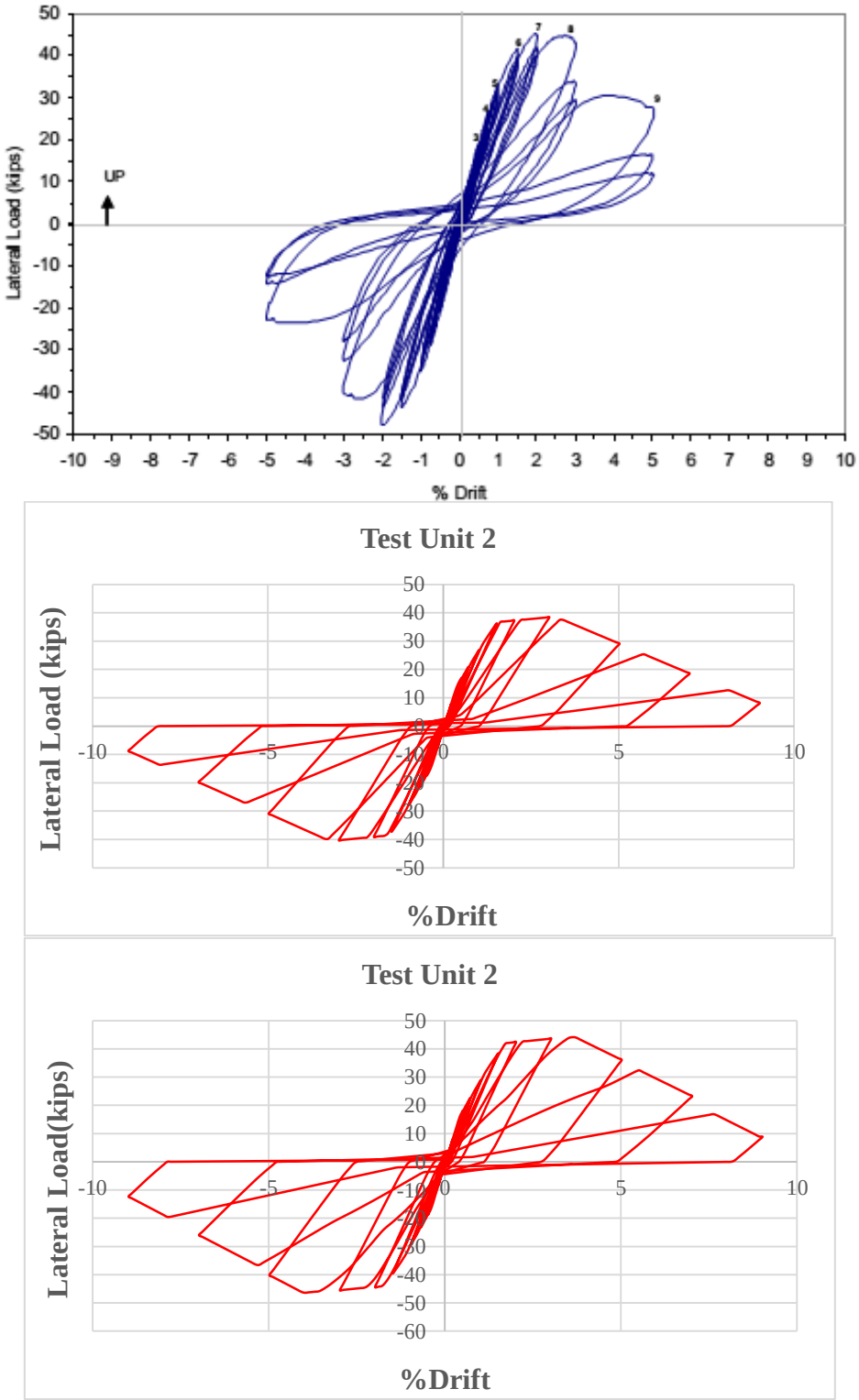

Fig 17. *Comparison of the graphs from the experimental data (top), data produced from the Kim and LaFave (2009) model (middle) and the data produced from the Jeon (2013) model (bottom) for test unit 2*

Test Unit 3

The plot (Figure 17) seen below shows the lateral load against drift as simulated by Opensees with a rotational spring joint model. It is easy to notice that both graphs somewhat resemble the experiment data in

Figure 13. The upward direction resistance is slightly larger compared to that in the downward direction, mainly due to the identical embedment of both the top and bottom bars in the column joint. In order to keep the difference between the upward and downward loads, the ratio between their peaks (1.03) was noted and applied in the stress-strain backbone curve of the pinching4 material.

The comparison of the maximum loads in either direction between the three of the experimental data, the data from Kim and LaFave (2009) and that from the Jeon (2013) model can be found in Table 9 below:

Table 9. Comparison of load and drift values obtained from both models to experimental values for test unit 3

	Upward Direction Maximum Load (kips)	%Drift	Downward Direction Maximum Load (kips)	%Drift
Experiment	44.40	3.00	43.10	2.00
Kim and Lafave (2009)	40.83	3.02	39.59	2.88
Jeon (2013)	47.78	4.52	46.29	4.28

By comparison, the values provided by Jeon (2013) joint shear strength prediction model are significantly closer to the experimental data.

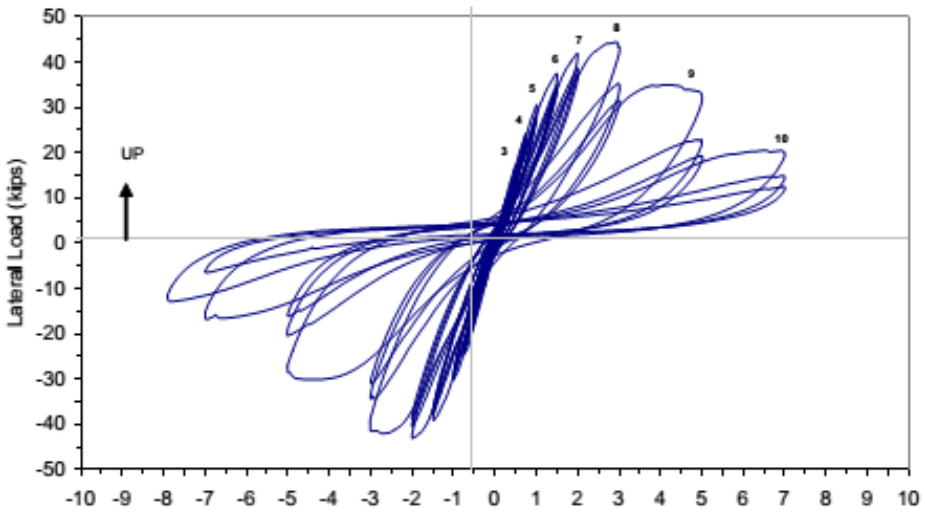

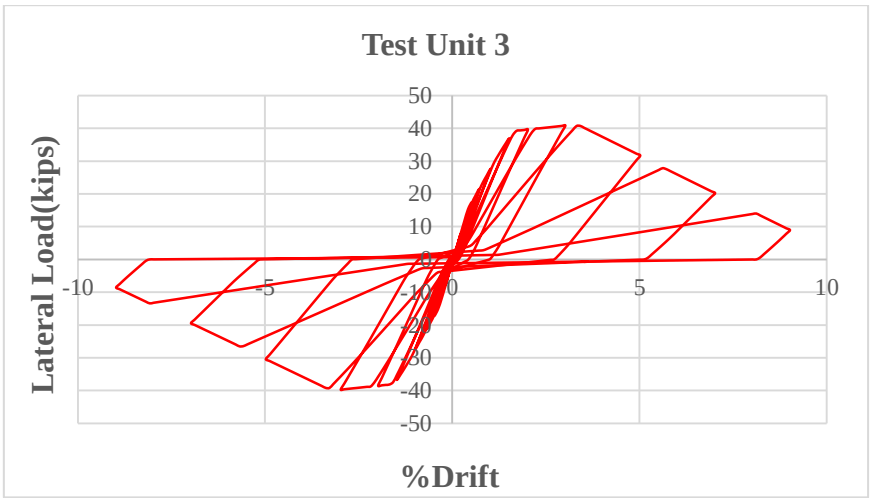

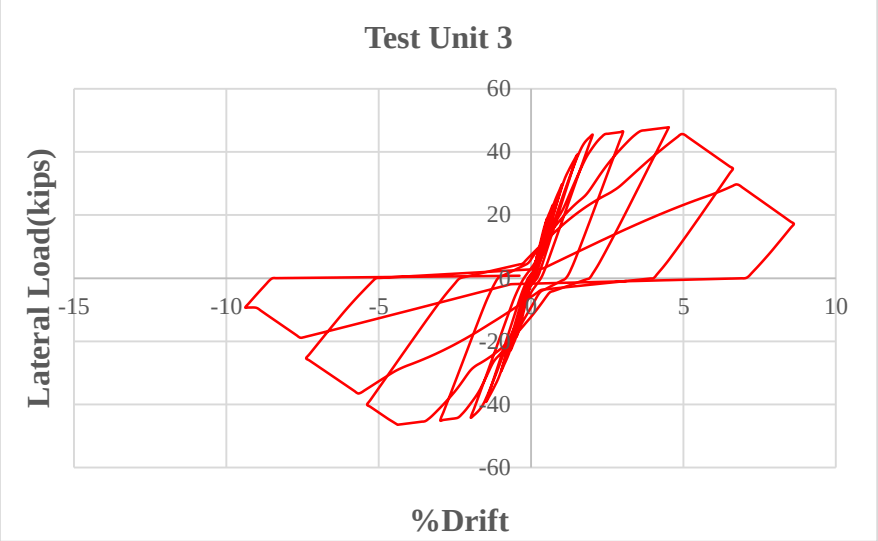

Fig 18. *Comparison of the graphs from the experimental data (top), data produced from the Kim and LaFave (2009) model (middle) and the data produced from the Jeon (2013) model (bottom) for test unit 3*

It can be seen in the above comparisons that while the models are very good for predicting lateral loads, the drift values are far from accurate with respect to the experimental data. This poses the thought that they are conservative models. But it might be possible to draw a favourable conclusion from analysing the lateral load values at the same drift at which maximum lateral load occurs for the experimental data and compare them. Table 10 below shows the comparison.

Table 10. *Comparison of peak lateral loads at the drifts at which the experimental peaks occur*

		Upward Direction		Downward Direction	
Test Unit	Dataset	Maximum Load (kips)	%Drift	Maximum Load (kips)	%Drift
1	Experiment	28.30	1.48	42.70	1.52
	Kim and Lafave (2009)	22.93	1.48	36.39	1.52
	Jeon (2013)	28.09	1.48	39.43	1.52
2	Experiment	45.10	2.00	47.50	2.00
	Kim and Lafave (2009)	37.27	2.00	36.22	2.00
	Jeon (2013)	42.39	2.00	41.22	2.00
3	Experiment	44.40	3.00	43.10	2.00
	Kim and Lafave (2009)	37.03	3.00	35.76	2.00
	Jeon (2013)	43.62	3.00	39.65	2.00

The comparison above shows that using the drift at maximum lateral load for comparison yields similar results in the sense that both models predict fairly similar values to the experimental data, but that from Jeon (2013) still yields more accurate results. The difference in this case is that whereas using the peak shear capacities to compare, the drift values from Jeon (2013) are slightly higher, whereas in the case of using drift at peak shear capacity, the values from Jeon (2013) are slightly lower. The values from

Kim and LaFave (2009) are lower than the experimental values in both cases.

Additional Modifications and Comparisons

Seeing how both models gave reasonable but not exactly 100% correct estimates of the maximum loads and drift at which they occur, we decided to change the shear strength values in the pinching4 material until we found the most suitable value that would give a 100% match with the experimental results. Findings for shear capacities were 0.78 ksi for test unit 1, 0.82 ksi for test unit 2 and 0.81 ksi for test unit 3. Again, direct comparison between calculated values from both models and these ideal values show that the model proposed by Jeon (2013) is indeed more accurate.

Notable discrepancies in the data produced by the models include the occurrence where the lateral load values from both rotational spring models are reasonably close to experimental values, but the drift values are not at all similar. It can be noted that the computed peak values of both forces and drifts in each test unit, while close to their experimental counterpart, is ultimately not the same in both directions. The explanation for these discrepancies is likely due to the errors in manufacturing of the test units which cause imperfections in the produced units. Another explanation is due to the embedment length of the bottom and top bars. It can be seen that for test unit 1, the embedment length of the bottom bars is 6 inches, which is far less than the required development length (calculated as 12.47 inches). Test unit 2 however, has an embedment length of 14 inches, which checks out as adequate. Test unit 3 has identical embedment length for both the top and bottom bars.

CONCLUSIONS

The overall aim of this study has been to evaluate existing empirical joint shear capacity models. By simulating responses of previously tested beam-column joint models using the non-linear finite element computation platform Opensees, the following deductions were made;

- The model proposed by Jeon (2013) for predicting the joint shear strength of various beam-column subassemblies is quite accurate in terms of maximum shear load and maximum drift as compared to those of Kim and LaFave (2009) when both are implemented by rotational spring model with pinching4 material model in Opensees.
- Both models do a good job of predicting peak lateral loads, but fall short when it comes to the drift at which they occur. As such, they can be used as conservative models, with the knowledge that they are not too accurate when it comes to drift.
- In using finite element analysis software like Opensees, rigid models are not very accurate in replicating the inelastic behaviour of concrete joints. A model with a rotational spring is better at doing this.

REFERENCES

1. Adom-Asamoah, M., Osei, B.J. (2016) '*Nonlinear seismic behaviour of a super 13-element reinforced concrete beam column joint model*', Earthquakes and Structures, 11(5), 905-924.
2. Altoontash, A. (2004) '*Simulation and damage models for performance assessment of reinforced concrete beam-column joints*' Ph.D. Thesis, Department of Civil and Environmental Engineering, Stanford University, CA.
3. Attaalla, S.A. (2004) *' General analytical model for normal shear stress of type 2 normal and high strength concrete beam-column joints'*,

ACI Structural Journal, Vol. 101, No. 1, pp. 65–75.

4. Aycardi, L. E., Mander, J. B. and Reinhorn, A. M. (1995) '*Seismic resistance of reinforced concrete frame structures designed for gravity loads: Experimental performance of subassemblages*', ACI Structural Journal, Vol. 91, No. 5, pp. 552–563.
5. Bracci, J. M., Reinhorn, A. M. and Mander, J. B. (1996) '*Seismic resistance of reinforced concrete frame structures designed for gravity loads: Performance of structural system*', ACI Structural Journal Vol. 92, No. 5, pp. 597–609.
6. Celik, O. C. and Ellingwood, B. R. (2008) '*Modeling Beam-Column Joints in Fragility Assessment of Gravity Load Designed Reinforced Concrete Frames Modeling Beam-Column Joints in Fragility*', Journal of Earthquake Engineering, Vol. 12, No. 3, pp. 357–381.
7. Hassan, W. M. (2011) '*Analytical and Experimental Assessment of Seismic Vulnerability of Beam-Column Joints without Transverse Reinforcement in Concrete Buildings*', Ph.D.Thesis, Department of Civil and Environmental Engineering, University of California, Berkeley, CA.
8. Jeon, J. S. (2013) '*Aftershock Vulnerability Assessment Of Damaged Reinforced Concrete Buildings In California*' Ph.D.Thesis, Department of Civil and Environmental Engineering, Georgia Institute of Technology, Georgia, USA.
9. Kim, J. and LaFave, J. M. (2009) '*Joint Shear Behavior of Reinforced Concrete Beam-Column Connections subjected to Seismic Lateral Loading*', . Report No. NSEL–020, Department of Civil and Environmental Engineering, University of Illinois at Urbana-Champaign, IL.
10. Lowes, L. N. and Altoontash, A. (2003) '*Modeling Reinforced-Concrete Beam-Column Joints Subjected to Cyclic Loading*', ASCE Journal of Structural Engineering, Vol. 129, No. 12, pp. 1686–1697.
11. Mitra, N. (2007) '*An analytical study of reinforced concrete beam-column joint behavior under seismic loading*', Ph.D. Thesis, Department of Civil and Environmental Engineering, University of Washington, Seattle, WA.
12. Pantelides, C.P., Hansen, J., Nadauld, J., and Reaveley, L.D. (2002) , '*Assessment of Reinforced Concrete Building Exterior Joints with Substandard Details Assessment of Reinforced Concrete Building Exterior Joints with Substandard Details*', PEER Report 2002/18, Pacific Earthquake Engineering Center, University of California, Berkeley, CA.
13. Park, S. and Mosalam, K.M. (2013) '*Experimental investigation of nonductile RC corner beam-column joints with floor slabs*', ASCE Journal of Structural Engineering,Vol. 139, No. 1, pp. 1–14.
14. Park, S. and Mosalam, K. M. (2012) '*Experimental and Analytical Studies on Reinforced Concrete Buildings with Seismically Vulnerable Beam- Column Joints*', Ph.D. Thesis, Department of Civil and Environmental Engineering, University of California, Berkeley, CA.